The changes in near-surface ozone and precursors at two nearby tropical sites during annular solar eclipse of 15 January 2010

I. A. Girach,[1] Prabha R. Nair,[1] Liji Mary David,[1] Prashant Hegde,[1] Manoj Kumar Mishra,[1] G. Mohan Kumar,[2] S. Murali Das,[2] N. Ojha,[3] and M. Naja[3]

Received 7 July 2011; revised 7 November 2011; accepted 11 November 2011; published 10 January 2012.

[1] Studies on the solar eclipse–induced changes in near-surface ozone and its precursors NO_x and CO were carried out at two nearby tropical coastal locations, Thumba (very close to the sea) and the Centre for Earth Science Studies (CESS), which is 4.5 km off the Thumba coast and with varying topography, during the annular eclipse of 15 January 2010. The surface ozone decreased by 12 and 13 ppb (35% and 52%) over Thumba and CESS, with the time lag of 40 min and 25 min from the maximum phase of eclipse, respectively, and at CESS, post-eclipse recovery was faster compared to Thumba. No pronounced change was observed in NO_x, but CO showed an enhancement toward the ending phase of the eclipse. The diurnal patterns of ozone and their differences at the two sites were strongly dependent on local meteorology, in particular, the mesoscale dynamics and topography. While the temperature decreased by 1.2°C at Thumba, the decrease was almost double (~2.1°C) at CESS. The early fall in temperature caused the early setting in of land-breeze (post-eclipse effect), which in turn triggered an early evening decrease in near-surface ozone compared to the control conditions. The present study points to the role of mesoscale meteorology/dynamics in controlling the evolution of solar eclipse–induced changes in ozone in a relatively clean environment. The chemical box model simulations reproduced these broad features: a percentage decrease and the time lag in surface ozone. The observation of total column ozone showed a decrease and fluctuations, after the eclipse maximum.

Citation: Girach, I. A., P. R. Nair, L. M. David, P. Hegde, M. K. Mishra, G. M. Kumar, S. M. Das, N. Ojha, and M. Naja (2012), The changes in near-surface ozone and precursors at two nearby tropical sites during annular solar eclipse of 15 January 2010, *J. Geophys. Res.*, *117*, D01303, doi:10.1029/2011JD016521.

1. Introduction

[2] The solar eclipse on 15 January 2010 was the longest annular eclipse of this millennium with 11 min 8 s of annularity and 0.919 of magnitude (http://eclipse.gsfc.nasa.gov/). Solar eclipse produces an abrupt and short-time variability in the magnitude and spectral characteristics of the solar radiation reaching the Earth unlike the changes that occur during a day to night transition which is relatively slow. The reduction in solar irradiance affects the photochemical as well as dynamical processes in the atmosphere significantly. Also, being a sudden and short-term phenomenon, the Earth's atmosphere and biosphere respond in different ways to it. Hence, the solar eclipse provides a unique opportunity to study the interactions between solar irradiance and the terrestrial atmosphere and the atmosphere's response to changes in solar forcing. The behavior of solar radiation at the Earth's surface during solar eclipse has been extensively investigated in the past by means of ground-based measurements [*Silverman and Mullen*, 1975; *Fernández et al.*, 1993a, 1993b; *Beletsky et al.*, 1998; *Mikhalev et al.*, 1999; *Zerefos et al.*, 2000, 2001; *Kazadzis et al.*, 2007; *Kazantzidis et al.*, 2007; *Krezhova et al.*, 2008]. There are several studies that report the solar eclipse–induced changes in spectral solar UV irradiance at the Earth's surface [*Fernández et al.*, 1993a; *Mikhalev et al.*, 1999; *Zerefos et al.*, 2000], surface temperature, winds [*Fernández et al.*, 1993b], mesoscale atmospheric circulation [*Gross and Hense*, 1999] vertical column abundance of atmospheric OH [*Burnett and Burnett*, 1985], etc. The decline of the direct solar irradiance at the shorter wavelengths is much more compared to the diffuse component during the eclipse [*Zerefos et al.*, 2001] and the reduction in UV irradiance is higher than that of the longer wavelengths [*Antón et al.*, 2010]. Model-based studies by *Chimonas and Hines* [1970] have shown that during solar eclipses, the movement of the cooled spot in the ozone layer can lead to the production of internal atmospheric gravity waves in the atmosphere. Later several authors provided

[1]Space Physics Laboratory, Vikram Sarabhai Space Centre, Thiruvananthapuram, India.
[2]Atmospheric Science Division, Centre for Earth Science Studies, Thiruvananthapuram, India.
[3]Aryabhatta Research Institute of Observational Sciences, Nainital, India.

0148-0227/12/2011JD016521

experimental observations of these waves during eclipse events [*Bertin et al.*, 1977; *Butcher et al.*, 1979; *Jones et al.*, 2004].

[3] Since solar eclipse creates a well-quantified and rapid modulation in solar intensity, it provides an excellent opportunity to probe atmospheric photochemistry. This is particularly true for atmospheric ozone since its production and destruction mechanisms are controlled by photochemistry involving several trace gases, in addition to meteorology and dynamics. In fact, the most efficient reactions involving ozone are driven by solar radiation [*Finlayson-Pitts and Pitts*, 2000; *Seinfeld and Pandis*, 2006]. The effects of a solar eclipse on the total ozone column have been widely studied by various groups [*Bojkov*, 1968; *Mims and Mims*, 1993; *Chakrabarty et al.*, 1997, 2001; *Zerefos et al.*, 2000; *Kazadzis et al.*, 2007; *Zerefos et al.*, 2000 and references therein]. A series of fluctuations in the column ozone was observed following the totality of eclipse preceded with reduced amplitude [*Mims and Mims*, 1993]. Column ozone measurements during the eclipse on August 11, 1999 showed positive and negative fluctuations of 2% in the column ozone within a period of two hours [*Tzanis*, 2005]. During the same eclipse, at the maximum obscuration, the ozone column has decreased by about 25 Dobson units (DU) from its pre-eclipse value over New Delhi (28.4N 77.1E) [*Chakrabarty et al.*, 1997, 2001]. Wavelike fluctuations were observed in total columnar ozone over Ahmedabad, India (23N, 72E).

[4] However, studies on the solar eclipse induced effects on surface ozone and its precursor gases like NO_x, CO, etc are limited particularly over the tropics. A decrease of 18–21% in surface ozone was observed at Ahmedabad during the maximum phase of the solar eclipse of 24 Oct 1995 [*Naja and Lal*, 1997] and that of ~11 to 12 ppbv at Robertsgunj 24°42′N, 83°04′E), compared to its concentration on control days [*Dani and Devara*, 2002]. It was also observed that during an eclipse, the surface OH concentration, which is critical in tropospheric chemistry, decreased dramatically to below 2.1×10^5 molecules cm^{-3} after maximum eclipse, and the concentration of ozone dropped to 60% of its value at first contact over the Silwood Park Atmospheric Research Station (51°25′N, 0°41′W) in Ascot [*Abram et al.*, 2000].

[5] This paper presents the observational results on the impact of the annular eclipse on January 15, 2010 on near-surface ozone and its precursor gases NO_x* (see section 3) and CO at two nearby tropical sites with varying topography/orography. A detailed account of the role of local meteorology and solar irradiance changes in the temporal evolution of ozone mixing ratio during eclipse is also given in this paper.

2. Eclipse and Experimental Sites

[6] Figure 1a shows the map depicting the solar eclipse path over Indian region where lines are labeled with duration of annularity or totality. Over the experimental location Thiruvananthapuram, the annular solar eclipse began at 11:05 IST, reached the maximum obscuration at 13:14 IST and ended at 15:05 IST. The duration of annularity and maximum obscurity were 07m16s and 84.3% (magnitude of 0.918), respectively, at this location, and the eclipse phenomenon lasted for ~2 h from first contact to fourth contact. In connection with the solar eclipse, measurements of near surface ozone, NO_x* and CO along with meteorological parameters were carried out at two nearby sites in Thiruvananthapuram (8.5°N, 76.9°E).

[7] The two experimental sites Thumba and CESS (Centre for Earth Science Studies) are marked in the map shown in Figure 1b. The site, Thumba, is situated just 500 m away from the Arabian Sea coast, with sandy terrain, and is a less populated area as can be seen in the figure. At this site, the strong sea-breeze (SB)/land breeze (LB) activity prevails during daytime, throughout the year [*Narayanan*, 1967; *David and Nair*, 2011]. The other site, CESS, is ~4.5 km inland and ~3.0 km away from the coast. CESS is highly vegetated site surrounded by small hilly terrain and experiences feeble sea-breeze as compared to Thumba. The city of Thiruvananthapuram with a population of ~3,234,356 (as per 2001 census) lies toward the eastern side of the experimental sites and is closer to CESS.

3. Instrumentation and Data

[8] The measurements of near-surface O_3, NO_x* ($NO+NO_2$*), and CO were carried out using the online UV photometric O_3 analyzer (Model O_3 42), chemiluminescent nitrogen oxide analyzer (Model AC32M) and gas filter correlation CO analyzer (Model CO12), respectively, of Environnement S.A, France. The measurements are being carried out at Thumba since February 2009 on the routine basis. In connection with the solar eclipse, pre-planned measurements of these gases were carried out in the campus of CESS from January 12 to 19 with identical instruments. The ozone analyzer works on the principle of ultraviolet absorption of ozone at the wavelength 253.7 nm. The instrument has a lower detection limit of 1 ppbv and 1% linearity. The nitrogen oxide measurement is based on the property of chemiluminescence of NO_2 molecules. The NO in the air first is oxidized by ozone (from an internal source) to form excited NO_2 molecules. Based on the measurement of luminous radiation, emitted by excited NO_2 molecules, in a 600–1200 nm spectrum the concentration of NO, NO_2 and NO_x are estimated. The NO_2 measurement is done after transforming them into NO under high temperature with Molybdenum converter. The instrument has a lower detection limit of 0.4 ppbv and 1% linearity. Although the conversion is about 100% efficient [*Winer et al.*, 1974; *Finlayson-Pitts and Pitts*, 1986], it is known that the molybdenum converter also converts other oxides of nitrogen such as PAN, HNO_3, etc. to NO [e.g., *Winer et al.*, 1974]. Thus, the actual concentrations of NO_2, and hence NO_x, may be lower than those measured. The NO_2 and NO_x measurements presented here should be considered as upper limits to its true values, and so they are represented here as NO_2* and NO_x*, respectively [*Naja and Lal*, 2002]. The CO analyzer works on the principle of infrared absorption of CO at the wavelength of 4.67 μm. The optical filter combined with a gas filter called 'correlation wheel', gives the highly selective measurement of CO gas by eliminating interference from any gas with absorption peak close to that of CO. The instrument has a lower detection limit of 50 ppbv and 1% linearity. An intercomparison for the respective analyzers was made at the same location, Thumba, by drawing air through the same inlet and found the measurements to be in good agreement. Prior to the

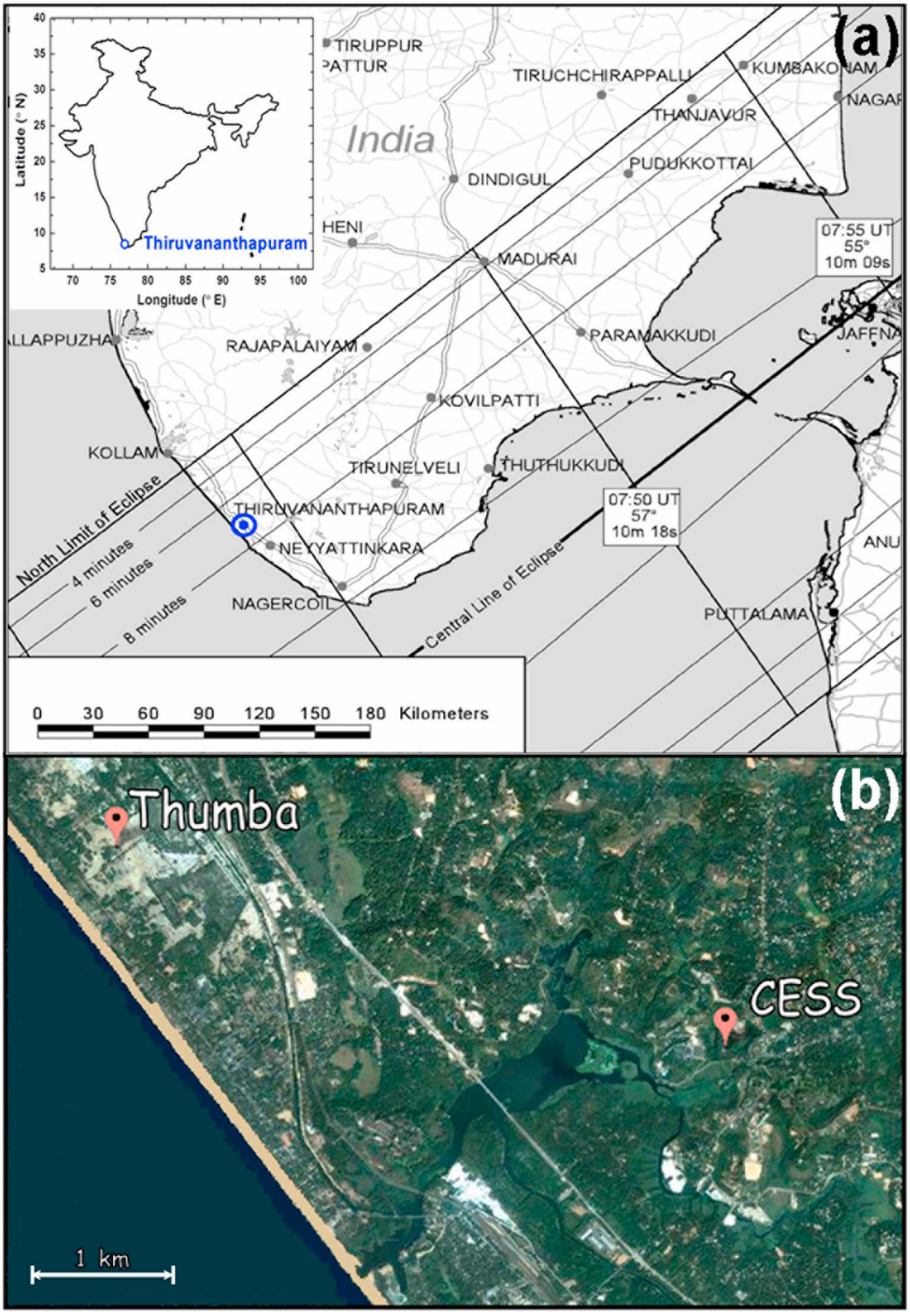

Figure 1. (a) Eclipse path passing over Thiruvananthapuram and (b) satellite image showing two different sites.

measurements, all the analyzers were calibrated using standard gas (traceable to NIST) diluted with custom-made calibrator. Data was recorded continuously at an interval of 5 min. For the present study, the data collected during the 8-day period of January 12–19, 2010 have been used. The meteorological parameters, namely temperature (T), relative humidity (RH), wind speed (WS), wind direction (WD) and total solar radiation (TSR) in W/m^2 were measured with 1 min time resolution at the experimental sites using Automatic Weather Stations. The TSR was measured by SP-Lite Silicon Pyronometer which makes global radiation measurement in the wide band of 400–1100 nm. Unfortunately, the wind

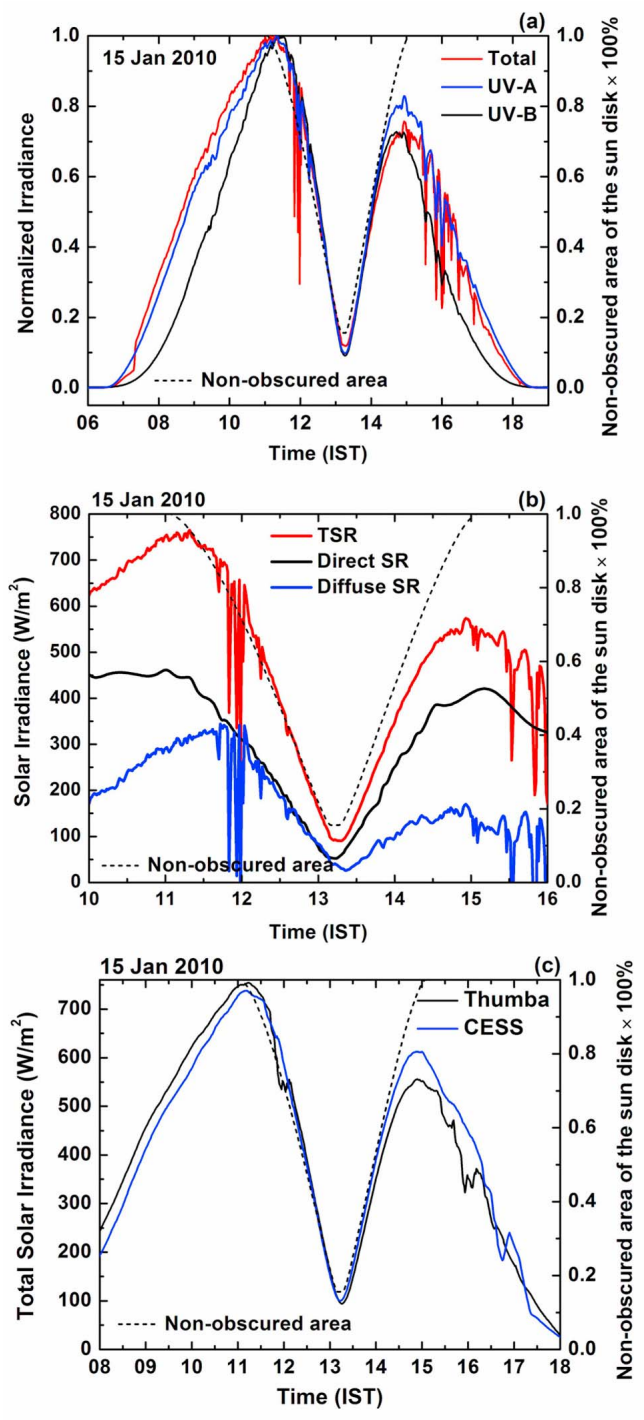

Figure 2. (a) Normalized irradiance UV-A, UV-B, and total solar radiation measured over Thumba; (b) direct, diffuse, and total solar irradiance measured over Thumba; and (c) total solar irradiance (smoothed) measured over Thumba and CESS.

direction measurements at CESS did not have high angular resolution. It was measured sector wise (45°). Total column ozone measurements were also done at Thumba using Microtops II Ozone Monitor and Sunphotometer (Solar Light Co., Inc, USA). This instrument derives total ozone column by measurement at three wavelengths, 300, 305.5 and 312.5 nm. In addition, measurements of global UV-A (315–400 nm) and UV-B (280–315 nm) were also carried out at Thumba with 1 min time resolution during eclipse period using UVS-AB-T Radiometer of Kipp and Zonen B. V., The Netherlands. This instrument became operational from 14 January 2010 only and UV-A, B measurements could not be conducted at CESS. In addition to this, ground reaching direct solar spectral irradiance in the band 350 to 2500 nm with the spectral resolution of 1 nm and a field of view of 2.5° was also measured during this period using FieldSpec-3 spectroradiometer of Analytical Spectral Device, Inc., Company (ASD Inc., USA). It was operated at 2–5 min intervals under clear sky conditions during eclipse time.

[9] Impacts of eclipse on the trace gases were investigated by comparing the eclipse day measurements of various parameters with that of non-eclipse days (control days). Since the meteorological conditions as well as trace gas concentrations exhibit large day to day variability, in the present study, control day parameters are taken as the average of 7 consecutive non eclipse days (from 12 to 19 January 2010 excluding 15 January, the eclipse day). Continuous measurements were available for both the sites for this period.

4. Results and Discussion

4.1. Solar Eclipse Induced Changes in Solar Irradiance on Ground

[10] Figure 2a shows the UV-A and UV-B irradiances along with TSR normalized to their maximum pre-eclipse value measured at Thumba on the solar eclipse day. The dotted lines in the figure represent the percentage obscurity. Solar irradiance at all the three wavelength bands started decreasing ~11:20 IST after the start of eclipse (first contact ~11:05). The minimum irradiance with 1 or 2 min time lag almost coincided with maximum obscuration (13:14 IST) and there after it increased along with the recovery phase of eclipse. The sudden change/fluctuations in UV-A and B around 12:00 IST is due to cloud patches. Toward the ending phase of eclipse also (1500–1700 IST) patches of clouds appeared, which is manifested as the fluctuations in irradiance. During the eclipse maximum, UV-A and UV-B decreased ~91% from its pre-eclipse value whereas the decrease in total solar irradiance was slightly less being 89% from its pre-eclipse value. Figure 2b shows the variation of direct and diffuse radiation along with TSR. The diffuse radiation was estimated by subtracting the direct radiation obtained using Spectroradiometer and integrated over 400–1100 nm, from TSR. The dip in direct radiation occurred exactly at the maximum obscuration as expected. The minimum diffuse radiation occurred at 13:20 with the time lag of 5–6 min from the maximum obscuration unlike in the earlier studies. In this context it is worth mentioning that the diffuse radiation is contributed by the multiple scattering effects from aerosols, cloud particles, etc., present in other parts of the atmosphere also. Hence it need not follow the declining pattern of direct solar irradiance. The possible explanation for the observed time lag in diffuse radiation could be the changes in the distribution of aerosols in the lower troposphere or their physical/chemical characteristics, all of which have dependence on meteorological parameters also. The

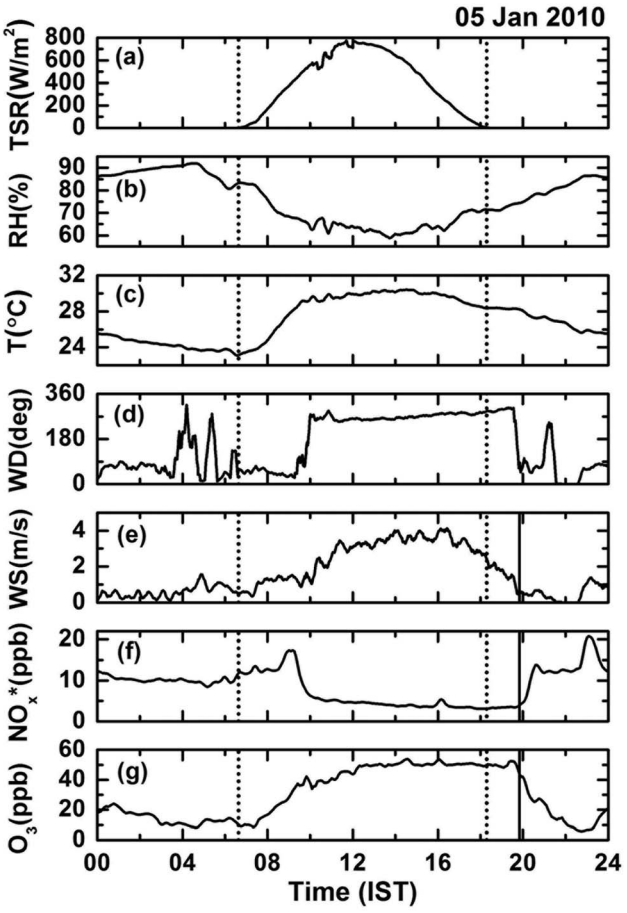

Figure 3. A typical diurnal pattern of (a) total solar irradiance (TSR), (b) relative humidity (RH), (c) temperature (T), (d) wind direction (WD), (e) wind speed (WS), (f) near-surface NO_x,* and (g) near-surface ozone over Thumba. Vertical lines in Figures 3e, 3f, and 3g are showing the onset of land breeze over the site. Dotted vertical lines represent the sunrise/sunset timings.

reduced convective mixing during eclipse enables confinement of aerosols to lower regions and also the increase in relative humidity (discussed in the section 4.4) promotes growth of particles (being a coastal site significant amount of hygroscopic particles are present in this location). The observed delay in the occurrence of minimum in diffuse radiation can be partly due to these effects. The measurements at Mount Athos have revealed that the reduction in diffuse component is less compared to that in the direct component during eclipse [*Zerefos et al.*, 2000]. Moreover, the ratio of diffuse to direct components in shorter wavelengths (e.g., 400–500 nm) peaks around the totality leaving the ratio unaffected in longer wavelengths. In Figure 2c is shown the comparison between the TSR measured at Thumba and CESS (since UV and spectral irradiance measurements are not available at CESS). At both these sites, the temporal variation of TSR showed a similar pattern during eclipse. But before the start of eclipse TSR was higher at Thumba and during post eclipse period it was higher at CESS. This could be due to the differences in atmospheric conditions, which causes changes in diffuse radiation.

[11] Decrease in solar irradiance during solar eclipses varies mainly with eclipse parameters like degree of obscuration, limb darkening effects, season, location, etc. During the solar eclipse on August 11, 1999 solar ultraviolet flux at Ascot (51°25′N, 0°41′W) has decreased to its nighttime levels [*Abram et al.*, 2000]. Prominent decrease in the UV irradiance at the lower wavelengths has also been reported [*Antón et al.*, 2010]. Measurements from a network of stations in Greece showed that reduction of irradiance at 305 and 312 nm relative to non-eclipse conditions was ∼1.5 times more than the corresponding decrease in the UV-A and visible part of the spectrum [*Kazantzidis et al.*, 2007].

[12] The following sections discuss how the above changes in solar irradiance caused by the eclipse affected the near-surface ozone, its precursor gases and the boundary layer meteorology.

4.2. Typical Diurnal Variation of Ozone and NO_x* Along With Meteorology Over Thumba

[13] As stated in section 2, the site Thumba experiences strong SB and LB activities. Note that at this location, the wind direction between 145 to 325° represents SB and beyond that denotes LB. Figure 3 shows the typical diurnal variation in ozone and NO_x* along with that of meteorological parameters WS, WD, temperature, RH and TSR over Thumba as measured on January 05, 2010. The diurnal pattern of ozone is characterized by day time high, which is attributed to photochemical production and nighttime low produced by the titration of ozone with NO_x* [*Nair et al.*, 2002; *David and Nair*, 2011]. After sunrise, photolysis reaction of NO_2 gets initiated and ozone concentration starts increasing as can be seen in the Figure 3g. Temperature is positively correlated with ozone (Figure 3c) and anti correlated with RH as expected. Along with photochemical production of ozone, destruction of ozone occurs via titration reaction of NO. These two competing processes decide the concentration of ozone during the daytime. Also SB is stronger compared to LB as seen by wind speed. During day time SB prevails over the site (Figure 3d) which brings relatively pristine air. With the sunset, photochemical production of ozone stops and destruction of ozone through titration becomes dominant. The unique feature of the site is that ozone does not decrease with the sunset, but it remains high until the onset of LB, which brings in NO_x* needed for titration with ozone thus leading to delay in the evening fall [*David and Nair*, 2011]. From Figure 3f it can be seen that the diurnal variation of NO_x* is opposite in nature to that of ozone with daytime low and nighttime high. From Figures 3a and 3d, it is clearly seen that the evening fall in ozone coincides exactly with the onset of LB.

4.3. Impact of Eclipse on Near-Surface Ozone and Precursor Gases

[14] Figures 4a and 4b show the diurnal pattern of ozone on eclipse day along with mean of control days (7 noneclipse days) for Thumba and CESS, respectively. From Figure 4 it can be seen that the daytime peak in ozone on the control day over CESS is low by ∼9 ppb compared to that at Thumba even though the two sites are separated by ∼4.5 km only. The reason for observed low ozone could be associated with the topography around this measurement site. It is a

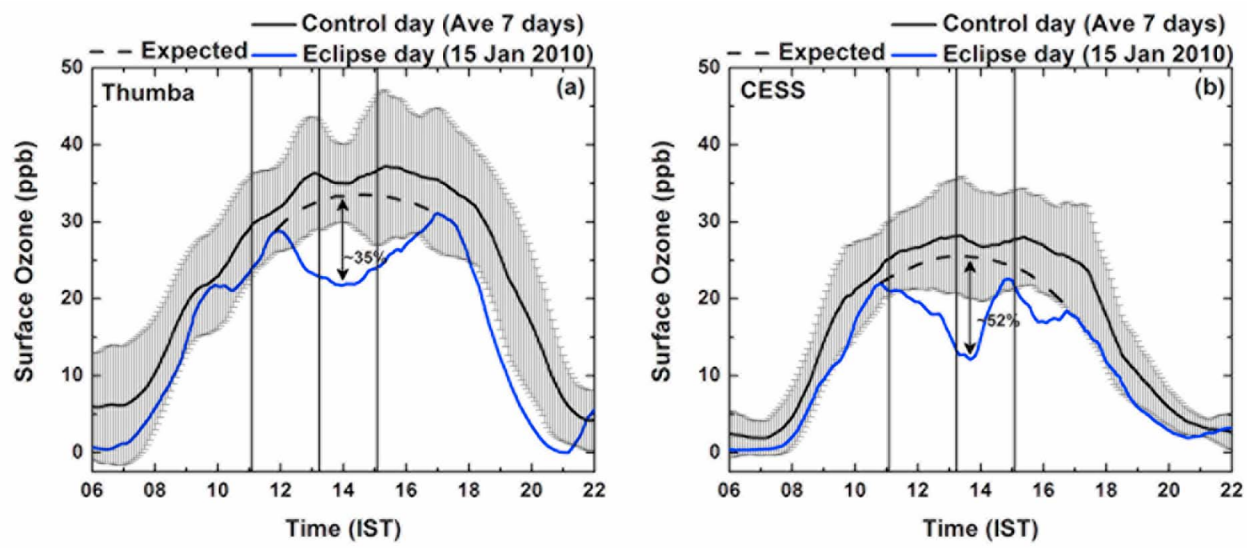

Figure 4. Near-surface ozone measured during eclipse and control days over (a) Thumba and (b) CESS. The vertical lines represent the first contact (left line), maximum phase (middle line), and last contact (right line).

highly vegetated terrain surrounded by small hilly regions also covered with vegetation. It is known that vegetation reduces the ozone level by the process of diffusion from the ambient air into the leaf through the stomata and this uptake is higher during the daytime as stomata are open during the day for photosynthesis [*Galbally and Roy*, 1980; *Butler and Tibbits*, 1979]. Moreover, the wind speed is low at this location (as seen from Figure 6j) inhibiting rapid transport of local pollutants (ozone precursors) to this site for the ozone production. Also, the level of NO_x* over CESS is lower as compared to that over Thumba. The low ozone concentration observed over CESS could be due to these reasons. Eclipse induced effect on surface ozone are clearly visible at both the sites. Solar eclipse causes significant reduction in ozone being well beyond the standard deviations (beyond the day to day variability). Since on eclipse day ozone level was lower as compared to control day and to attribute the correct loss of ozone due to eclipse, the decrease in ozone was calculated with respect to the dashed line (drawn manually) as shown in the Figure 4. Irrespective of the difference in control day ozone levels, the eclipse induced decrease in ozone is more or less similar being ∼12 to 13 ppb at both the sites. In this context, it is worth mentioning that the total solar irradiance decreased by ∼85% at both the sites (Figures 6a and 6f). It is also important that the percentage decrease is different at the two sites, being 35% at Thumba and 52% at CESS. The decrease in ozone was also estimated with respect to the control day value (mean of 7 days) considering standard deviations corresponding to the time of eclipse maximum which is 8 to 18 ppb (27%–46%) over Thumba and 8 to 23 ppb (40%–65%) over CESS. In addition, the decrease in ozone did not start with the first contact at Thumba as it can be seen from Figure 4a. Ozone continued to increase reaching 28 ppb around 12:00 IST and then started decreasing slowly showing a broad minimum.

[15] Since the site, Thumba is very close to sea, thus it experiences stronger influences of SB/LB activities in comparison with CESS (as seen from Figure 6). Moreover, the low wind speed facilitates confinement of pollutants over the site. Thus the variations in ozone and precursors at Thumba are more influenced by the mesoscale dynamics while those at CESS, which is significantly inland (∼3 km away from sea), by the in situ photochemistry. Due to this, similar reduction in solar radiation is capable of more reduction in ozone at CESS (52%) than that at Thumba (35%). Also, since photochemistry is perturbed instantaneously, thus the effect of eclipse is observed immediately on the ozone levels at CESS while it is significantly delayed (∼40 min) at Thumba.

[16] As eclipse progressed, ozone attained its minimum value of 21 ppb around 13:55 IST with the time lag of ∼40 min with respect to maximum obscuration (which was at ∼13:15 IST). After that ozone started recovering and reached 31 ppb around 17:00 IST. A decrease of ∼22% is seen during eclipse with respect to the 12:00 value. On the other hand, at the site CESS, decrease in ozone (21 ppb at first contact) started almost coinciding with the start of eclipse (Figure 4b). Ozone decreased by 9 ppb reaching 12 ppb (∼42% decrease) around 13:40 (IST) with time lag of 25 min with respect to the maximum eclipse. The time lag in attaining dip represents the slow destruction process. Ozone recovered very fast and maximized to 23 ppb at 14:50 IST just around the ending phase of eclipse unlike at Thumba, where recovery also was delayed. It can be noted that the minimum in ozone does not coincide with the time of maximum solar obscuration and there is the time lag in attaining minimum at both the stations. The differences in the evolution of solar eclipse induced changes at these two sites are attributed to the varying impact of mesoscale circulation (SB/LB) and the availability of precursor gases. These aspects are discussed in detail later in this section. In connection with the same eclipse, *Sharma et al.* [2010] conducted measurement of O_3, NO_x, CO, etc. close to the city ∼6 km from the coast in a relatively polluted environment (0.5 km away from national highway, NH 47). The observed values of all these species were higher than

those recorded at the coastal and unpolluted sites. Also they observed increase in NO associated with the eclipse induced reduction in ozone (of ~20 ppb) which is attributed to source effects. The observation of Ozone and NO_x at another site, Kannur (11.9°N, 75.4°E) in the western coastal belt of India and close to national highway, recorded 57.5% decrease during eclipse along with 62.5% increase of NO_x [*Nishanth et al.*, 2011].

[17] Studies conducted at various locations over the globe have revealed that solar eclipse causes changes of different magnitudes and temporal scales in ozone. The observed decrease in near-surface ozone due to solar eclipse of 24 October 1995 was ~11 to 12 ppbv at Robertsgunj (24°42′N, 83°04′E). At Ahmedabad (23.05°N, 72.67°E) decrease in ozone concentration observed at the maximum phase of eclipse of 24 October 1995 was about 18%–21% [*Naja and Lal*, 1997]. The solar eclipse of 11 August 1999, was a well-studied event in terms of the number of experiments and spatial coverage [*Abram et al.*, 2000; *Chudzynski et al.*, 2001; *Fabian et al.*, 2001; *Farges et al.*, 2003; *Jones et al.*, 2004, *Koepke et al.*, 2001; *Kolarž et al.*, 2005; *Szalowski*, 2002; *Tzanis*, 2005; *Zanis et al.*, 2001; *Zerefos et al.*, 2000, 2001]. Ozone decrease of ~8 ppb (from 22 to 14 ppb) was observed over Silwood Park, Ascot (51°25′N, 0° 41′W) during the eclipse [*Abram et al.*, 2000]. Model based study by *Fabian et al.* [2001] has shown the reduction in net O_3 production by 4–5 ppbv. The decrease in surface ozone can be attributed to the abrupt reduction in solar radiation at shorter wavelengths that affects photochemical reactions. *Fabian et al.* [2001] has also reported an increase of 10 ppb in the ozone concentration during the totality of the eclipse of 11 August 1999 which could be partly explained by photochemistry, which can account for the 30 percent increase of the species. While the surface ozone measurements showed a decrease of ~10 to 15 ppbv at the urban station, at an elevated rural site it did not show any clear effect of eclipse [*Zanis et al.*, 2001; *Zerefos et al.*, 2001]. All these indicate the influence of other parameters/factors controlling the eclipse produced changes in ozone in addition to direct photochemistry. The present study indicates that at the coastal site Thumba, which is relatively unpolluted, the mesoscale circulation plays a significant role in the evolution of eclipse induced changes in the surface ozone.

[18] Time lag in attaining minimum concentration, similar to that observed in the present study, is also reported from other sites, which was attributed to reasons like slow destruction processes, photochemical relaxation time, etc. For example, the maximum percentage change in surface ozone was observed one hour after the maximum of the solar eclipse at four stations in Greece during the solar eclipse of 29 March 2006 [*Tzanis et al.*, 2008]. The observed time lags in the decrease of ozone level as well as in the occurrence of minimum from maximum phase of eclipse indicate the slow ozone destruction processes. However, it is obvious that the eclipse induced changes in ozone and precursors strongly depend on the location, proximity to sources and meteorology. These aspects need to be investigated in detail.

[19] Ozone level at any location is controlled by (1) photo chemical oxidation of precursor gases and (2) prevailing meteorological conditions and dynamics.

[20] Solar radiation contributes to tropospheric ozone through several reactions of varying rate constants and pathways. In presence of NO_2, majority of ozone in the boundary layer is formed through photochemical reactions given by the equations,

$$NO_2 + h\nu \rightarrow O(^3P) + NO(\lambda < 424\ \text{nm}) \quad (1)$$

$$O(^3P) + O_2 + M \rightarrow O_3 + M \quad (2)$$

$$O_3 + NO \rightarrow NO_2 + O_2 \quad (3)$$

Excited O (^{1}D) (Photolysis of ozone at $\lambda < 320$ nm leads to production of excited state O (^{1}D)) collides with H_2O producing OH radicals which converts NO to NO_2 as given by following equations.

$$O(^1D) + H_2O \rightarrow 2OH \quad (4)$$

$$OH + CO \rightarrow H + CO_2 \quad (5)$$

$$H + O_2 + M \rightarrow HO_2 + M \quad (6)$$

$$HO_2 + NO \rightarrow OH + NO_2 \quad (7)$$

[21] These reactions and hence the tropospheric ozone budget is controlled primarily by the $j_{O(1D)}$ and j_{NO2} rate constants and NO_x and HO_2 budgets. The immediate effect of eclipse is the reduction of j_{NO2} which perturbs the steady state condition. The decrease in ozone during eclipse is related to the fall in production rate from the oxidation reactions discussed above. As totality is approached, due to decreasing solar flux, photolysis of NO_2 (reaction 1) weakens/stops and consequently, concentration of O_3 will keep on decreasing. In addition, during eclipse period, loss processes including ozone titration by NO_x can also decrease the ozone levels, depending on the availability of NO_x. While the eclipse associated reduction in radiation is ~85%, the observed reduction in surface ozone from the pre-eclipse value is ~22%. The time lag between the ozone minimum and the eclipse maximum is partly related to the relaxation time of the photostationary state, which is of the order of few minutes [*Seinfeld and Pandis*, 2006]. However, for the difference in the time lag observed at Thumba and CESS (which are very closely situated and where the radiation changes are similar), the meteorological conditions along with perturbations in boundary layer dynamics could have caused the temporal shifts. Like photochemical production, destruction of ozone is also strongly influenced by the amount of NO_x available. In the absence of photolysis of NO_2, NO needed for titration has to be produced in situ by anthropogenic sources or transported from nearby populated areas. But no strong sources of NO exist in and around Thumba. Due to the strong SB prevailing at Thumba and absence of local sources, the air is relatively pollutant (NO_x) free during daytime which restricts the photochemical destruction. That is why ozone remains high even after sunset till the onset of LB, which brings NO_x for titration as seen in Figure 3 and discussed in detail by *David and Nair* [2011]. Moreover, the already available ozone gets circulated in the SB cell. As the observation site, CESS is

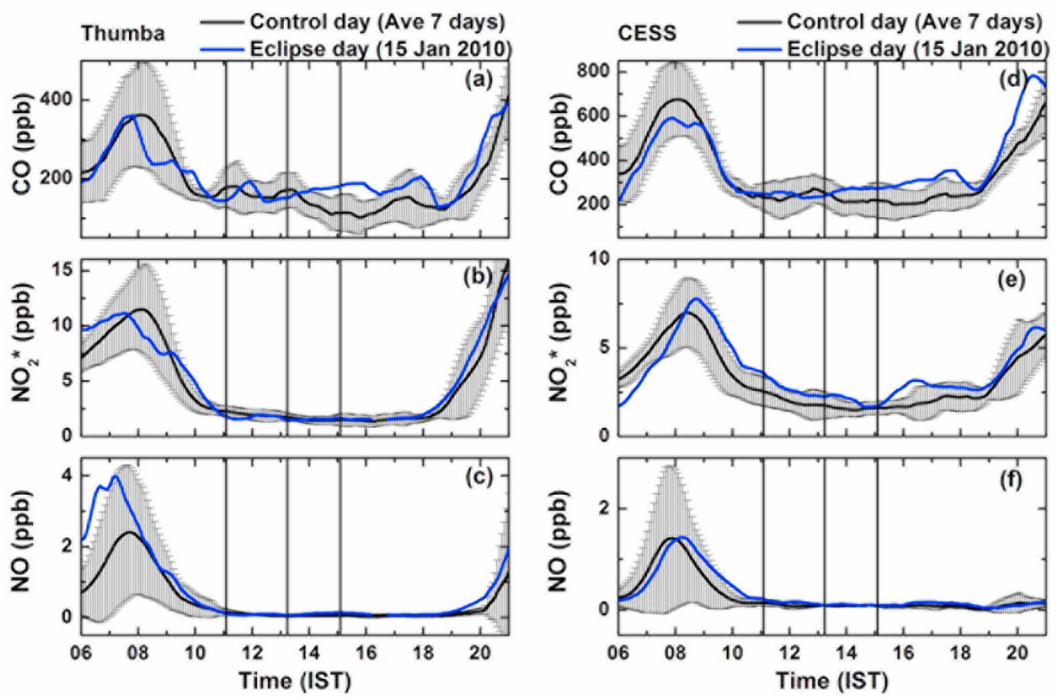

Figure 5. Near-surface (a and d) carbon monoxide, (b and e) nitrogen dioxide, and (c and f) nitric oxide measured over Thumba (Figures 5a–5c) and CESS (Figures 5d–5f) during eclipse and control days. The vertical lines represent the first contact (left line), maximum phase (middle line), and last contact (right line).

surrounded by hilly terrain and winds are weak pollutant gases get confined over the site and have longer residence times. This may be why the lag in attaining minimum at CESS is ~15 min earlier compared to Thumba. The high NO_x values observed over here during nighttime is due to transport from polluted inland by the LB activity.

[22] During eclipse, since production of O_3 through photolysis of NO_2 gets weakened /stopped, build-up of NO_2 can be expected. In fact, at most of inland (more polluted) sites, build-up of NO_2 is observed with the decrease in ozone. Figure 5 shows the diurnal variation of NO and NO_2* on eclipse day along with those for the control period estimated as in the case of ozone (Figure 5) for both the experimental sites. It is clearly seen from Figures 5b, 5c, 5e, and 5f that there was no significant change in NO/NO_2* concentration during initial phase of eclipse till its maximum phase (as the values are within the day to day variability). This could be due to the fact that NO_2* level was at low. During day time sea breeze prevails bringing in pristine marine air mass with less/no pollutant gases and there are no local sources also. However, basic photochemical reactions take place during daytime (in low NO_2 conditions) contributing to O_3 balance. Due to scarcity of NO during daytime, reaction (3) is insignificant and hence increase in NO_2 during the obscuration is not observed. So whatever depletion we observe in ozone is caused by the reduction in photo chemical production and direct photochemical destruction of ozone rather than titration by NO_x chemistry. That is why no build-up is observed in NO_x during eclipse unlike in the case of polluted sites. In general build-up of NO_2, associated with decrease in ozone, is observed at polluted sites [*Zanis et al.*, 2007]. This occurs when the primary pollutant NO destroys ozone through the titration reaction (3) without ozone being produced through the photolysis reaction (1). Significant reduction in UV-B (91%) during maximum phase of eclipse decelerates the O (^{1}D) induced OH production and subsequent regeneration of NO_2. However, after the eclipse maximum, the NO_2* showed an increasing trend at CESS. An increase of 1.3 ppb (73%) in NO_2* was observed during the post eclipse period at CESS around (15:30 to 16:45 IST).

[23] The photolysis and oxidation reactions of other species like CO, CH_4 and VOCs also contribute to ozone concentration at any location, particularly polluted environments. OH radicals as well as NO_2 play major roles in these reactions and acting as a sink for these species. The reaction sequence of ozone production from CO is given below.

$$CO + OH + O_2 \rightarrow CO_2 + HO_2 \quad (8)$$

$$HO_2 + NO \rightarrow NO_2 + OH \quad (9)$$

$$NO_2 + h\nu + O_2 \rightarrow O_3 + NO \quad (10)$$

$$\text{Net} : CO + 2O_2 + h\nu \rightarrow CO_2 + O_3 \quad (11)$$

[24] As it can be seen from the above reactions, it is obvious that the production of O_3 through this channel is also driven by solar radiation which gets depleted during eclipse. This can result in build-up of CO. The temporal behavior of CO on eclipse day is shown in Figures 5a and 5d along with that of the control day for Thumba and CESS. CO shows a slightly different picture from that of O_3 and NO_x* on eclipse day. During eclipse period no significant change is noticed in CO as in the case of NO_x*. However, an

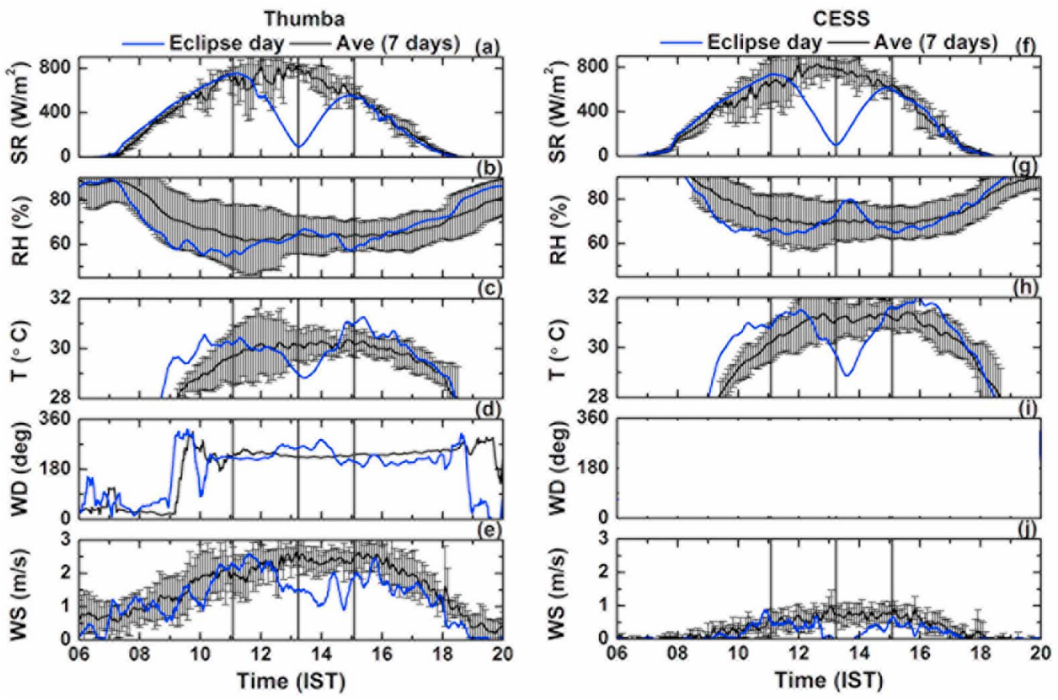

Figure 6. (a and f) Solar irradiance, (b and g) relative humidity, (c and h) temperature, (d and i) wind direction, and (e and j) wind speed observed at Thumba (Figures 6a–6e) and CESS (Figures 6f–6j) during the eclipse of 15 January 2010. All the parameters are compared with its averaged value over 7 days. The error bar shows the standard deviation in the respective parameter. The vertical lines represent the first contact (left line), maximum phase (middle line), and last contact (right line).

increase of 85 ppb (∼81%) and 115 ppb (∼48%) were observed at Thumba and CESS around the ending phase of eclipse (14:15 to 16:25 IST and 15:35 to 18:10 IST), respectively. Photochemical box model was run to simulate this effect using the observed diurnal variation of O_3, NO_x, water vapor and other meteorological parameters. Since no simultaneous measurements were available on CH_4 and other hydrocarbons, earlier CH_4 data from this site [*Lal et al.*, 2004] and data for other species as given by *Finlayson-Pitts and Pitts* [2000] were used for the simulation. Even though the model is capable of producing the broad features (qualitatively) of the diurnal pattern like the daytime decrease, it could not reproduce the enhancement of CO observed toward the end of eclipse. This indicates that it is not directly driven by $O_3/NO_x/OH$ chemistry. But the model simulation also indicated that certain hydrocarbons can promote production of CO. Hence the observed increase in CO could be either due to some local sources of CO or its precursor hydrocarbons. However, this needs further investigations. Solar eclipses enable the evaluation of response of the gas-phase chemistry of photo-oxidants during a drastic perturbation in solar radiation. A detailed account of the chemical effects of the solar eclipse of 29 March 2006 on surface ozone and other photo-oxidants at four sites in Greece with different pollution levels is given by *Zanis et al.* [2007]. In these studies, the coastal sites where NO and NO_2 levels were low, no clear impact of solar eclipse on the surface O_3, NO_2 and NO concentrations was seen from the observations as well as model simulations. At polluted urban/suburban sites where ozone levels were 30–42 ppb and 30–50 ppb, respectively, solar eclipse effects on O_3, NO_2 and NO concentrations were clearly indicated from both the measurements and 3-D air-quality modeling. In the present study, near-surface ozone is found to decrease significantly during eclipse, while the precursor concentrations were not affected much. This is attributed to the relatively clean conditions at these locations with lower levels of pollutants like NO_x, CO, etc. The eclipse induced reduction in ozone can be mainly due to photochemistry. The amplitude of depletion and the time lag in attaining minimum are modified/controlled by local meteorology in particular the mesoscale circulation. The variations in boundary layer height and perturbations in the associated mixing can also contribute to the observed changes.

4.4. Changes in Meteorological Parameters

[25] The production, destruction and transport of gases and pollutants in the atmospheric boundary layer (ABL) are controlled by the meteorological conditions, in particular, by wind, RH, temperature and variations in boundary layer height. A change in the radiative forcing of the atmosphere is manifested first in the ABL where turbulence processes dominate. Figures 6a–6j show the impact of the solar eclipse on meteorological parameters, namely relative humidity, temperature, wind direction and wind speed along with TSR, observed at Thumba and CESS. Though two sites are separated only by 4.5 km, this figure shows that the diurnal variation of the meteorological parameters were distinctly different in terms of humidity, temperature and wind. Being coastal locations these sites experience SB/LB activity as discussed in section 4.2. Since CESS is ∼3 km away from sea and has small hilly regions around, it experiences weaker SB (as can be seen from the daytime low wind speed)

whereas the site, Thumba experiences strong SB/LB activity. Temperature at this site is lower compared to CESS.

[26] Total solar radiation showed a decrease of ~85% at both the sites. This drastic change in solar radiation resulted in pronounced changes in surface air temperature. It is also noted that the drop in temperature is not analogous to that of solar irradiance which is proportional to percentage obscuration. On the other hand, it depends on several local factors like time of the day, latitude of location, season, the synoptic conditions, the height of measurements, the climatic and other local features (e.g., topography, vegetation, soil conductivity), and so on, rather than eclipse parameters. In general, the temperature drop becomes noticeable when the sun is about half-covered [*Anderson*, 1999]. The magnitude of temperature drop also varies with local conditions. However, immediate response as well as delayed response of temperature has also been reported by various observers [*Anderson and Keefer*, 1975; *Szalowski*, 2002; *Narasimha et al.*, 1982]. The air temperature was decreased by 1.2°C (with 13 min time lag from the maximum phase of eclipse) and 2.1°C (with 25 min time lag) over Thumba and CESS, respectively. It is important to see that though two sites are separated only by 4.5 km, the difference in decease in temperature is almost double (1.2 to 2.1). Temperature drop ranged from 2.3°C to 2.7°C with the time lag of 12–14 min from maximum phase of the eclipse have been reported earlier during solar eclipse on 26 March 2006 [*Founda et al.*, 2007]. Temperature decrease of 5.8°–2.5° was observed with the corresponding increase of 15%–7% in RH over Gadanki (13.51°N, 79.21°E), a tropical rural station, during the eclipse of 15 January 2010 [*Venkat Ratnam et al.*, 2010]. The time lag between the occurrences of the temperature minimum and the maximum phase of eclipse is considered to be the result of the thermal inertia of the air and the ground [*Fernández et al.*, 1993b]. The observed differences in the temperature drop at the two sites could be contributed by several factors, including meteorological conditions and surface properties. The proximity to sea (having a large heat capacity) and the relatively strong winds might have blocked the temperature at the surface level from falling to lower values at Thumba. The observation point at CESS is more distant from sea and also surrounded by land. Moreover calm wind conditions prevailed over CESS preventing mixing of surface air as can be seen from wind speed. As a consequence of temperature drop, RH is expected to rise. In the present study, even though the RH increase is not very large still it is showing some tendency of increasing (Figures 6b and 6g). The anticorrelation of the temperature and RH in Figures 8b and 8g indicate that the absolute water vapor content did not change significantly during the eclipse. Hence, the OH driven reaction series given by equations (4)–(7) will also be weak. This can slow down the regeneration of NO_2.

[27] Associated with solar eclipse, decrease in surface wind speed was also observed at several locations [*Founda et al.*, 2007; *Gerasopoulos et al.*, 2008]. At Thumba, wind speed decreased to 1.1 m/s from its pre-eclipse value of 2.2 m/s at ~13:55 IST, 40 min after the maximum phase. It is interesting to note that ozone minimum also showed a similar time lag with respect to eclipse maximum. It is also seen that wind direction changed 35–40 (wind became southwesterly to westerly) over Thumba during 12:40 to 14:20 h. The change in wind direction toward the direction of the shadow motion was reported earlier also [*Dolas et al.*, 2002; *Stove et al.*, 2005]. At CESS, wind speed was 0.5 m/s at first contact and became nearly zero at ~12:55 which remained for 1 h duration (12:55 to 14:00) and started increasing afterwards. At this location, no change could be observed in wind direction during eclipse probably because of the coarse resolution measurements/due to relatively complex topography of the site (surrounded by small hilly regions). The deceleration of wind flow observed during solar eclipse [e.g., *Fernández et al.*, 1993a, 1993b; *Dolas et al.*, 2002; *Krishnan et al.*, 2004; *Stove et al.*, 2005] is attributed to the combined effect of the decrease of the thermal gradient, the stabilization of surface layer (due to decrease in temperature) and the suppression of turbulent processes.

[28] The observed changes in ozone over CESS match with the pattern of cut-off of the radiation the precursor concentration remaining almost constant. The calm wind condition over CESS during eclipse inhibits/slows down transport of ozone/NO_x produced around. Lower wind speed over CESS during maximum phase of eclipse made the confined/laboratory condition. Thus, the sharp dip in ozone at CESS could be due to photochemistry. The higher time lag as well as broadness in dip observed over Thumba is attributed to dynamics since nonzero wind speed can bring in/recirculate locally generated ozone and precursors (local transport). The SB cell prevailing at this coastal site is responsible for the recirculation [*David and Nair*, 2011].

[29] Another striking feature seen from Figure 4 that the evening decrease of ozone starts early compared to control days. In this context, the diurnal pattern of air temperature (Figures 6c and 6h) was also examined. As seen from Figure 7, temperature also started decreasing early (16:00) on the eclipse day compared to the control days (which is at 18:00 h). Moreover, eclipse night was relatively cool as compared to the control night with the temperature remaining low till next day morning (Figure 7). As a result, land breeze also started early at Thumba as compared to control day as shown in Figure 6d. It is reported that at Thumba the evening decrease of ozone is closely associated with the onset of LB [*David and Nair*, 2011]. The site being relatively free of anthropogenic activities and SB (relatively clean air) prevails during the daytime, for titration of ozone to occur LB has to onset bringing in NO_x as reported by *David and Nair* [2011]. In this context, it is interesting to note that the evening decrease in ozone started early on the eclipse day, also coinciding with the onset of LB. As mentioned earlier wind direction measurement over CESS did not have the fine angular resolution (it was measured sector wise) exact time of SB to LB transition could not be seen. However, at CESS also evening decrease of ozone started early. The early fall in the ozone concentration in evening due to eclipse is one of the important results of this study. These investigations point to the role of mesoscale meteorology and in particular, dynamics in controlling the diurnal variations in near surface ozone and its precursors.

4.5. Model Simulations

[30] A chemical box (zero-dimensional) model, NCAR Master Mechanism (NCAR-MM), developed at National

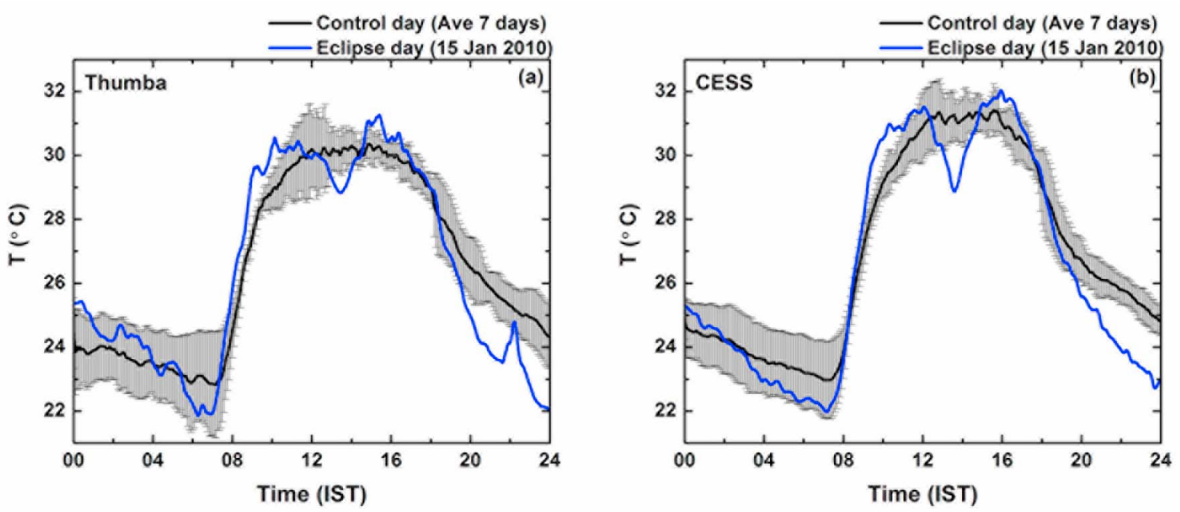

Figure 7. Temperature variation on eclipse day over (a) Thumba and (b) CESS.

Center for Atmospheric Research, Boulder, USA [*Madronich and Calvert*, 1990; *Madronich and Flocke*, 1999] was used to study the eclipse effect on surface ozone. The model simulates chemical evolution of an air parcel taking into account the detailed gas phase chemistry. The estimation of photolysis rate coefficients is done using the Tropospheric Ultraviolet Visible (TUV) radiative transfer model with a 4-stream discrete ordinate radiative transfer solver [*Stamnes et al.*, 1988]. More details of NCAR-MM are given by *Madronich* [2006]. The environmental conditions used for the model simulation are given the Table 1.

[31] The initial/background concentrations of CH_4, CH_2O, isoprene, C_3H_6 and i-butane were taken as 1.7 ppm, 5, 5, 5 and 4 ppb, respectively, which represent the typical coastal/rural conditions. While the background values of ozone, NO, NO_x were the nighttime averaged values i.e., 4, 0.3, 3.5 ppb, the initial values of that were observed values at 0 h (i.e., 6 ppb for ozone). The crucial diurnal constraints used in the simulation were the observed temperature, humidity, NO, NO_2, and CO. Observed NO_2 diurnal values were used in the simulation giving an offset of 1.1 ppb taking into account the over estimation in the measurement of NO_2 due to molybdenum convertor and performing sensitivity simulations. The boundary layer variation of 0.2 km during the night to 2 km during the day was assumed in the present simulation. For the eclipse simulation, the time evolution of solar obscurity is introduced in the model while all other input parameters were kept to their values of normal simulation. The fractional obscurity was calculated from the observed radiation pattern. The model simulated diurnal variation of ozone along with the observed diurnal pattern on the eclipse day is shown in Figure 8a. It can be seen that the model reproduced the overall variations reasonably well; however, there are differences in the absolute levels of ozone. Figure 8b shows the diurnal pattern of ozone on eclipse day simulated with and without eclipse effect. The eclipse produced depletion in the ozone is 33%. This is in reasonable agreement with the observed reduction in ozone (~35%) during the maximum phase of eclipse. Interestingly, time lag (with respect to maximum obscuration) produced by model coincides with the observation.

[32] The model simulation shows that ozone didn't recover to its pre-eclipse value even after the end of eclipse. It is worth mentioning that model does not account for transport and dynamics. Moreover, at this coastal site, mesoscale circulations (sea breeze and land breeze) strongly affect the diurnal pattern of ozone and its precursors [*David and Nair*, 2011]. The slow recovery of ozone to pre-eclipse value could be partially attributed to dynamics. The delay produced by slow wind and wind direction changes in bringing in the ozone/precursors may be partially responsible for the observed variation in surface-ozone. Also no additional emissions, dilution and heterogeneous processes are assumed in the present model simulation. The decrease and time-lag are attributed to purely photochemistry, which became less active during the cut-off of the radiation.

4.6. Impact of Solar Eclipse on Columnar Ozone

[33] In connection with solar eclipse, measurements of total column ozone were also carried out at Thumba using Microtops II Ozone Monitor/Sunphotometer [Solar Light Co, USA]. Microtops II makes measurement of directly transmitted ground reaching solar UV radiation at 300, 305.5, and 312.5 nm and by taking the ratio at two

Table 1. The Major Environmental Parameter Used for Box Model Simulations

Parameter	Value
Latitude, longitude	8.5°N, 76.9°E
Date	15 Jan 2010
Parcel elevation	50 m
Ozone column	260 DU (Microtop II observation)
AOD at 550 nm	0.370 (typical value during January at Thumba)
Aerosol SSA	0.730 (typical value during January at Thumba)
Aerosol Angstrom coefficient	1.012 (typical value during January at Thumba)
Temperature	299.5 K (observed average value)
Air density	2.449×10^{19} molecules/cm^3
Relative humidity	78% (observed level)

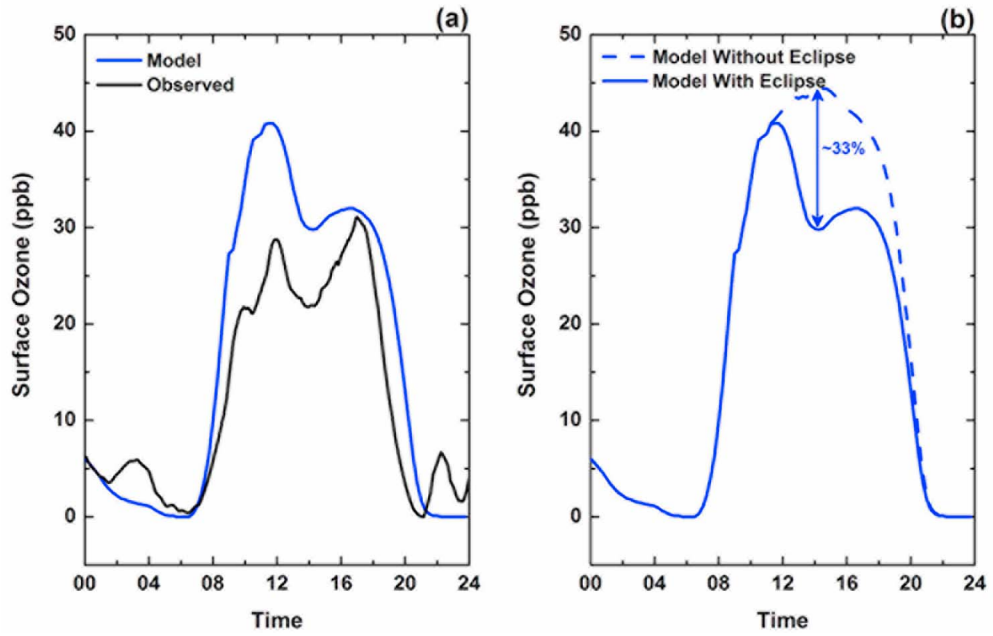

Figure 8. (a) Observed and model-simulated diurnal variation of surface ozone for the eclipse day. (b) Model-simulated diurnal variation of surface ozone with and without eclipse effect.

wavelengths for retrieval of column ozone [*Morys et al.*, 2001]. Hence, the measurement of ozone is independent of the absolute amount of radiation. It is known that limb darkening effect of sun results in apparent increase in column ozone. Even applying corrections, several groups detected eclipse induced changes in column ozone and showed that the short-term fluctuations are not an artifact of this instrumental error [*Mims and Mims*, 1993]. *Zerefos et al.* [2001] suggested that the error due to limb darkening effect is less than 1%. Later on, *Kazadzis et al.* [2007] computed the correction for total ozone which found to be much smaller (<0.01%). Another possible error in the sun-photometric measurement is that caused by diffuse radiation entering the instrument. From the simulations done for this tropical site, the estimated contribution of diffuse radiation for the 2.5° field of view of the instrument is ∼2%–3%. The decrease in column ozone caused by this diffuse component will not be significant, even though there can be an artifact. However, the observed fluctuations can be treated as reliable as reported by *Mims and Mims* [1993]. Hence the present measurements using Microtops is used to derive a qualitative assessment of the changes in column ozone associated with the eclipse rather that a quantitative estimate. In addition, even when 84.4% radiation was cut off during eclipse, intensity of visible radiation was sufficient to focus the instrument toward the sun disk during the eclipse.

[34] Figure 9 shows the columnar ozone concentration measured during eclipse and control days. The gap in the data is because of presence of clouds around 12:00 IST which can be seen in Figure 2. With respect to control day measurements, 265 DU at 11:15, columnar ozone decreased by ∼16 DU reaching 249 DU. But as mentioned earlier, ozone itself was low on eclipse day, and hence it is better to see the changes with respect to its pre-eclipse value on the same day. The columnar ozone decreased by 14 DU from its pre-eclipse value (∼11:00 IST). Just after the maximum phase of eclipse undulation in columnar ozone was seen the periodicity of which is ∼ 20 min (Periodicity can be seen from the arrows marked in the Figure 9). Here, it is to be noted that these fluctuations started prior to the appearance of patchy clouds, that is by ∼15:00 IST (Figure 2). The undulations observed in columnar ozone concentration are of significant amplitude. The similar kinds of undulations were also reported in literature [*Mims and Mims*, 1993;

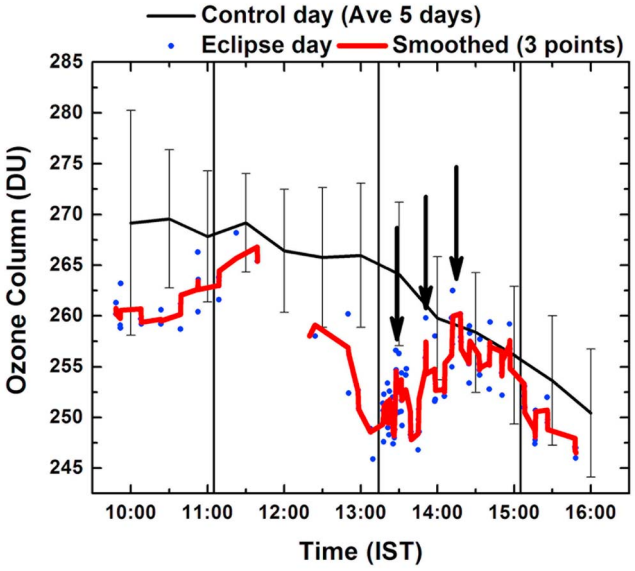

Figure 9. Columnar ozone concentration during eclipse day and control day, which is averaged over 5 days, measured over Thumba. The vertical bars represent the standard deviation. The dark vertical lines represent the first contact (left line), maximum phase (middle line), and last contact (right line). The three arrows represent the undulations.

Chakrabarty et al., 1997, 2001]. The similar variation in ground-reaching UV radiation is expected due to increase and decrease in total columnar ozone. But UV-A or UV-B did not show any undulation during 13:00 to 15:00 h. This probably due to UV-A or UV-B is broadband global measurement. However, these are only broad qualitative features and needs further analysis.

5. Conclusions

[35] The measurements of near-surface ozone, NO_x*, CO along with meteorological parameters and solar irradiance were made during annular eclipse on 15 January 2010 over two nearby coastal sites, Thumba which is very close to sea and CESS which is ~4.5km off Thumba coast having different topographic/orographic features. In addition, measurements of ground-reaching UV-A, UV-B, direct solar irradiance, and columnar ozone were also done. The major results of this study are summarized below.

[36] 1. The eclipse induced decrease in near-surface ozone was ~12–13 ppb at both the sites. But the percentage decrease from the control day condition was 35% and 52% with the time lag of 40 min and 25 min over Thumba and CESS, respectively. The presence of time lag represents the slow process of ozone destruction. The higher time lag observed over Thumba is attributed to the stronger effect of the prevailing mesoscale circulation (sea breeze). The rate of recovery was faster over CESS as compared to Thumba and ozone recovered to its pre-eclipse value coinciding with the end of the eclipse.

[37] 2. The maximum decrease in direct solar irradiance occurred with maximum obscuration but the dip of diffuse radiation occurred with 5–6 min time lag. This is attributed to changes in aerosol distribution/characteristics.

[38] 3. Due to the cut-off of radiation, temperature and wind speed were also affected significantly. While the temperature decreased by 1.2°C at Thumba, it was almost twice (2.1°C) at CESS with the respective time lags being 13 and 25 min. The wind speed decreased by 1.2 m/s with the 40 min time lag over Thumba whereas wind became nearly zero over CESS from its pre-eclipsed value of 0.6 m/s. The change in wind direction was ~ 35° over Thumba.

[39] 4. Due to the early decrease in temperature the land breeze set in early on the eclipse night. With the onset of land breeze, ozone also showed early evening fall which is a post-eclipse effect.

[40] 5. No pronounced change was observed in the concentration of NO_x* during eclipse. However, CO showed an enhancement toward the ending phase of eclipse which could not be attributed fully to the effect of eclipse.

[41] 6. The decrease in surface ozone estimated by chemical box model was 33%, which is comparable with the observed decrease at Thumba. The box model has also reproduced the time lag. The model estimated recovery indicates the crucial role of mesoscale dynamics and boundary layer variations in controlling the recovery of ozone.

[42] 7. The measurements of columnar ozone from Microtops II Ozone Monitor showed a decrease of 14 DU. After the maximum phase of eclipse, the columnar ozone showed fluctuations of ~20 min, indicating the presence of wave activity. However, this needs further study.

[43] **Acknowledgments.** Authors acknowledge former director, T. Radhakrishnan, and head of the Atmospheric Science Division, N. Shubhas, at CESS for providing facilities and support to operate the instruments at CESS. The authors acknowledge D. Bala Subrahamanyam and N. V. P. Kiran Kumar for providing meteorological data recorded during the eclipse period.

References

Abram, J. P., D. J. Creasey, D. E. Heard, J. D. Lee, and M. J. Pilling (2000), Hydroxyl radical and ozone measurements in England during the solar eclipse of 11 August 1999, *Geophys. Res. Lett.*, *27*(21), 3437–3440, doi:10.1029/2000GL012164.

Anderson, J. (1999), Meteorological changes during a solar eclipse, *Weather*, *54*(7), 207–215.

Anderson, R. C., and D. R. Keefer (1975), Observations of temperature and pressure changes during the 30 June 1973 solar eclipse, *J. Appl. Meteorol.*, *32*, 229–231.

Antón, M., A. Serrano, M. L. Cancillo, J. M. Vaquero, and J. M. Vilaplana (2010), Solar irradiance and total ozone over El Arenosillo (Spain) during the solar eclipse of 3 October 2005, *J. Atmos. Sol. Terr. Phys.*, *72*, 789–793, doi:10.1016/j.jastp.2010.03.025.

Beletsky, A. B., A. V. Mikhalev, and M. A. Chernigovskaya (1998), Spectral measurements of the solar nearground UV radiation during the solar eclipse on March 9, 1997, *Atmos. Oceanic Opt.*, *11*, 301–306.

Bertin, K., F. A. Hughes, and L. Kersley (1977), Atmospheric waves induced by the solar eclipse of 30 June 1973, *J. Atmos. Sol. Terr. Phys.*, *39*, 457–461, doi:10.1016/0021-9169(77)90153-2.

Bojkov, R. D. (1968), The ozone variations during the solar eclipse of 20 May 1966, *Tellus*, *20*, 417–421, doi:10.1111/j.2153-3490.1968.tb00382.x.

Burnett, C. R., and E. B. Burnett (1985), Atmospheric hydroxyl response to the partial solar eclipse of May 30 1984, *Geophys. Res. Lett.*, *12*(5), 263–266, doi:10.1029/GL012i005p00263.

Butcher, E. C., A. M. Downing, and K. D. Cole (1979), Wavelike variations in the *F* region in the path of totality of the eclipse of 23 October 1976, *J. Atmos. Sol. Terr. Phys.*, *41*, 439–444, doi:10.1016/0021-9169(79)90068-0.

Butler, L. K., and T. W. Tibbits (1979), Stomata1 mechanisms determining genetic resistance to ozone in *Phaseolus uulgaris* L., *J. Am. Soc. Hort. Sci.*, *104*, 213–216.

Chakrabarty, D. K., N. C. Shah, and K. V. Pandya (1997), Fluctuation in ozone column over Ahmedabad during the solar eclipse of 24 October 1995, *Geophys. Res. Lett.*, *24*(23), 3001–3003, doi:10.1029/97GL03016.

Chakrabarty, D. K., S. K. Peshin, S. K. Srivastav, N. C. Shah, and K. V. Pandya (2001), Further evidence of total ozone variation during the solar eclipse of 1995, *J. Geophys. Res.*, *106*(D3), 3213–3218, doi:10.1029/2000JD900522.

Chimonas, G., and C. O. Hines (1970), Atmospheric gravity waves induced by a solar eclipse, *J. Geophys. Res.*, *75*(4), 875, doi:10.1029/JA075i004p00875.

Chudzynski, S., et al. (2001), Observation of ozone concentration during the solar eclipse, *Atmos. Res.*, *57*, 43–49, doi:10.1016/S0169-8095(00)00071-5.

Dani, K. K., and P. C. S. Devara (2002), Aerosol optical depth and ozone variations during the total solar eclipse of 24 October 1995, *Atmos. Res.*, *65*, 1–15, doi:10.1016/S0169-8095(02)00143-6.

David, L. M., and P. R. Nair (2011), Diurnal and seasonal variability of surface ozone and NO_x at a tropical coastal site: Association with mesoscale and synoptic meteorological conditions, *J. Geophys. Res.*, *116*, D10303, doi:10.1029/2010JD015076.

Dolas, P. M., R. Ramchandran, K. S. Gupta, S. M. Patil, and P. N. Jadhav (2002), Atmospheric surface-layer processes during the total solar eclipse of 11 August 1999, *Boundary Layer Meteorol.*, *104*, 445–461, doi:10.1023/A:1016577306546.

Fabian, P., et al. (2001), Boundary layer photochemistry during a total solar eclipse, *Meteorol. Z.*, *10*(3), 187–192, doi:10.1127/0941-2948/2001/0010-0187.

Farges, T., A. Le Pichon, E. Blanc, S. Perez, and B. Alcoverro (2003), Response of the lower atmosphere and the ionosphere to the eclipse of August 11, 1999, *J. Atmos. Sol. Terr. Phys.*, *65*, 717–726, doi:10.1016/S1364-6826(03)00078-6.

Fernández, W., V. Castro, J. Wright, H. Hidalgo, and A. Sáenz (1993a), Changes in solar irradiance and atmospheric turbidity in Costa Rica during the total solar eclipse of July 11, 1991, *Earth Moon Planets*, *63*(2), 119–132, doi:10.1007/BF00575101.

Fernández, W., V. Castro, and H. Hidalgo (1993b), Air temperature and wind changes in Costa Rica during the total solar eclipse of July 11, 1991, *Earth Moon Planets*, *63*, 133–147, doi:10.1007/BF00575102.

Finlayson-Pitts, B. J., and J. N. Pitts (1986), Formation of sulfuric and nitric acids in acid rain and fogs, in *Atmospheric Chemistry: Fundamental and Experimental Techniques*, edited by B. J. Finlayson-Pitts and J. N. Pitts, pp. 702–705, John Wiley, Hoboken, N. J.

Finlayson-Pitts, B. J., and J. N. Pitts Jr. (2000), *Chemistry of the Upper and Lower Atmosphere: Theory, Experiments, and Applications*, Academic, London.

Founda, D., D. Melas, S. Lykoudis, I. Lisaridis, E. Gerasopoulos, G. Kouvarakis, M. Petrakis, and C. Zerefos (2007), The effect of the total solar eclipse of 29 March 2006 on meteorological variables in Greece, *Atmos. Chem. Phys.*, *7*, 5543–5553, doi:10.5194/acp-7-5543-2007.

Galbally, I. E., and C. R. Roy (1980), Destruction of ozone at the Earth's surface, *Q. J. R. Meteorol. Soc.*, *106*, 599–620, doi:10.1002/qj.49710644915.

Gerasopoulos, E., et al. (2008), The total solar eclipse of March 2006: Overview, *Atmos. Chem. Phys.*, *8*, 5205–5220, doi:10.5194/acp-8-5205-2008.

Gross, P., and A. Hense (1999), Effects of a total solar eclipse on the mesoscale atmospheric circulation over Europe: A model experiment, *Meteorol. Atmos. Phys.*, *71*, 229–242, doi:10.1007/s007030050057.

Jones, T. B., D. M. Wright, J. Milner, T. K. Yeoman, T. Reid, P. J. Chapman, and A. Senior (2004), The detection of atmospheric waves produced by the total solar eclipse of 11 August 1999, *J. Atmos. Sol. Terr. Phys.*, *66*, 363–374, doi:10.1016/j.jastp.2004.01.029.

Kazadzis, S., A. Bais, M. Blumthaler, A. Webb, N. Kouremeti, R. Kift, B. Schallhart, and A. Kazantzidis (2007), Effects of total solar eclipse of 29 March 2006 on surface radiation, *Atmos. Chem. Phys.*, *7*, 5775–5783, doi:10.5194/acp-7-5775-2007.

Kazantzidis, A., A. F. Bais, C. Emde, S. Kazadzis, and C. S. Zerefos (2007), Attenuation of global ultraviolet and visible irradiance over Greece during the total solar eclipse of 29 March 2006, *Atmos. Chem. Phys.*, *7*, 5959–5969, doi:10.5194/acp-7-5959-2007.

Koepke, P., J. Reuder, and J. Schween (2001), Spectral variation of the solar radiation during an eclipse, *Meteorol. Z.*, *10*(3), 179–186, doi:10.1127/0941-2948/2001/0010-0179.

Kolarž, P., J. Šekarić, B. P. Marinković, and D. M. Filipović (2005), Correlation between some of the meteorological parameters measured during the partial solar eclipse, 11 August 1999, *J. Atmos. Sol. Terr. Phys.*, *67*, 1357–1364, doi:10.1016/j.jastp.2005.07.016.

Krezhova, D. D., A. H. Krumov, and T. K. Yanev (2008), Spectral investigations of the solar radiation during the total solar eclipse on March 29, 2006, *J. Atmos. Sol. Terr. Phys.*, *70*, 365–370, doi:10.1016/j.jastp.2007.08.057.

Krishnan, P., P. K. Kunhikrishnan, S. Muraleedharan Nair, S. Ravindran, R. Ramachandran, D. B. Subrahamanyam, and M. Venkata Ramana (2004), Observations of the atmospheric surface layer parameters over a semi arid region during the solar eclipse of August 11th, 1999, *Proc. Indian Acad. Sci.*, *113*, 353–363.

Lal, S., D. Chand, S. Venkataramani, K. S. Appu, M. Naja, and P. K. Patra (2004), Trends in methane and sulfur hexafluoride at a tropical coastal site, Thumba (8.6°N, 77°E), in India, *Atmos. Environ.*, *38*, 1145–1151, doi:10.1016/j.atmosenv.2003.11.019.

Madronich, S. (2006), Chemical evolution of gaseous air pollutants downwind of tropical megacities: Mexico City case study, *Atmos. Environ.*, *40*, 6012–6018, doi:10.1016/j.atmosenv.2005.08.047.

Madronich, S., and J. G. Calvert (1990), Permutation reactions of organic peroxy radicals in the troposphere, *J. Geophys. Res.*, *95*(D5), 5697–5715, doi:10.1029/JD095iD05p05697.

Madronich, S., and S. Flocke (1999), The role of solar radiation in atmospheric chemistry, in *Handbook of Environmental Chemistry*, edited by P. Boule, pp. 1–26, Springer, Heidelberg, Germany.

Mikhalev, A. V., M. A. Chernigovskaya, A. B. Beletsky, E. S. Kazimirovsky, and O. M. Pirog (1999), Variations of the ground measured solar ultraviolet radiation during the solar eclipse on March 9, 1997, *Adv. Space Res.*, *24*(5), 611–619, doi:10.1016/S0273-1177(99)00209-4.

Mims, F. M., III, and E. R. Mims (1993), Fluctuations in column ozone during the total solar eclipse of July 11, 1991, *Geophys. Res. Lett.*, *20*(5), 367–370, doi:10.1029/93GL00493.

Morys, M., F. M. Mims III, S. Hagerup, S. E. Anderson, A. Baker, J. Kia, and T. Walkup (2001), Design, calibration, and performance of MICROTOPS II handheld ozone monitor and Sun photometer, *J. Geophys. Res.*, *106*(D13), 14,573–14,582, doi:10.1029/2001JD900103.

Nair, P. R., D. Chand, S. Lal, K. S. Modh, M. Naja, K. Parameshswaran, S. Ravindran, and S. Venkataramani (2002), Temporal variations in surface ozone at Thumba (8.6°N, 77°E): A tropical coastal site in India, *Atmos. Environ.*, *36*, 603–610, doi:10.1016/S1352-2310(01)00527-1.

Naja, M., and S. Lal (1997), Solar eclipse induced changes in surface ozone at Ahmedabad, *Indian J. Radio Space Phys.*, *26*(6), 312–318.

Naja, M., and S. Lal (2002), Surface ozone and precursor gases at Gadanki (13.5°N, 79.2°E), a tropical rural site in India, *J. Geophys. Res.*, *107*(D14), 4197, doi:10.1029/2001JD000357.

Narasimha, R., A. Prabhu, K. Narahari Rao, and C. R. Prasad (1982), Atmospheric boundary layer experiment, *Proc. INSA Bull.*, *48*, 175–186.

Narayanan, V. (1967), An observational study of sea breeze at an equatorial coastal station, *Indian J. Meteorol. Geophys.*, *18*, 497–504.

Nishanth, T., N. Ojha, M. K. Satheesh Kumar, and M. Naja (2011), Influence of solar eclipse of 15 January 2010 on surface ozone, *Atmos. Environ.*, *45*, 1752–1758, doi:10.1016/j.atmosenv.2010.12.034.

Seinfeld, J. H., and S. N. Pandis (2006), *Atmospheric Chemistry and Physics: From Air Pollution to Climate Change*, 2nd ed., Wiley-Intersci., New York.

Sharma, S. K., et al. (2010), Effects of solar eclipse on 15 January 2010 on the surface O_3, NO, NO_2, NH_3, CO mixing ratio and the meteorological parameters at Thiruvanathapuram, India, *Ann. Geophys.*, *28*, 1199–1205, doi:10.5194/angeo-28-1199-2010.

Silverman, S. M., and E. G. Mullen (1975), Sky brightness during eclipses: A review, *Appl. Opt.*, *14*, 2838–2843.

Stamnes, K., S.-C. Tsay, W. J. Wiscombe, and K. Jayaweera (1988), Numerically stable algorithm for discrete-ordinate-method radiative transfer in multiple scattering and emitting layered media, *Appl. Opt.*, *27*, 2502–2509, doi:10.1364/AO.27.002502.

Stove, A., P. Stoeva, D. Valev, N. Kishkinova, and T. Tasheva (2005), Dynamics of the microclimatic parameters of the ground atmospheric layer during the total solar eclipse on August 11, 1999, *Geophys. Res. Abstr.*, *7*, 10,209.

Szalowski, K. (2002), The effect of the solar eclipse on the air temperature near the ground, *J. Atmos. Sol. Terr. Phys.*, *64*, 1589–1600, doi:10.1016/S1364-6826(02)00134-7.

Tzanis, C. (2005), Ground-based observations of ozone at Athens, Greece during the solar eclipse of 1999, *Int. J. Remote Sens.*, *26*, 3585–3596, doi:10.1080/01431160500076947.

Tzanis, C., C. Varotsos, and L. Viras (2008), Impacts of the solar eclipse of 29 March 2006 on the surface ozone concentration, the solar ultraviolet radiation and the meteorological parameters at Athens, Greece, *Atmos. Chem. Phys.*, *8*, 425–430, doi:10.5194/acp-8-425-2008.

Venkat Ratnam, M., M. S. Kumar, G. Basha, V. K. Anandan, and A. Jayaraman (2010), Effect of the annular solar eclipse of 15 January 2010 on the lower atmospheric boundary layer over a tropical rural station, *J. Atmos. Sol. Terr. Phys.*, *72*, 1393–1400, doi:10.1016/j.jastp.2010.10.009.

Winer, A. M., J. W. Peters, J. P. Smith, and J. N. Pitts Jr. (1974), Response of commercial chemiluminescent NO-NO_2 analyzers to other nitrogen-containing compounds, *Environ. Sci. Technol.*, *8*, 1118–1121, doi:10.1021/es60098a004.

Zanis, P., C. S. Zerefos, S. Gilge, D. Melas, D. Balis, I. Ziomas, E. Gerasopoulos, P. Tzoumaka, U. Kaminski, and W. Fricke (2001), Comparison of measured and modeled surface ozone concentrations at two different sites in Europe during the solar eclipse on August 11, 1999, *Atmos. Environ.*, *35*, 4663–4673, doi:10.1016/S1352-2310(01)00116-9.

Zanis, P., et al. (2007), Effects on surface atmospheric photo-oxidants over Greece during the total solar eclipse event of 29 March 2006, *Atmos. Chem. Phys.*, *7*, 6061–6073, doi:10.5194/acp-7-6061-2007.

Zerefos, C. S., et al. (2000), Changes in surface UV solar irradiance and total ozone during the solar eclipse of August 11, 1999, *J. Geophys. Res.*, *105*(D21), 26,463–26,473, doi:10.1029/2000JD900412.

Zerefos, C. S., et al. (2001), Changes in surface UV solar irradiance and ozone over the Balkans during the eclipse of 11 August 1999, *Adv. Space Res.*, *27*(12), 1955–1963, doi:10.1016/S0273-1177(01)00279-4.

S. M. Das and G. M. Kumar, Atmospheric Science Division, Centre for Earth Science Studies, Thiruvananthapuram, Kerala 695 031, India.

L. M. David, I. A. Girach, P. Hegde, M. K. Mishra, and P. R. Nair, Space Physics Laboratory, Vikram Sarabhai Space Centre, Thiruvananthapuram, Kerala 695 022, India. (imran.girach@gmail.com)

M. Naja and N. Ojha, Aryabhatta Research Institute of Observational Sciences, Manora Peak, Nainital, Uttaranchal 263129, India.